Trans. JSASS Aerospace Tech. Japan
Vol. 12, No. ists29, pp. Po_2_29-Po_2_38, 2014

Original Paper

Study of the Effects of Density, Thickness and Heat Load on Heat Shielding Performance of Phenolic Carbon Ablators Using a One-Dimensional Ablation Analysis Code

By Sumio KATO[1)], Takuya KISHIMOTO[1)], Shoichi MATSUDA[1)], Keiichi OKUYAMA[2)], Akihiro WATANABE[1)] and Naoyuki SHIMADA[1)]

[1)]*University of the Ryukyus, Okinawa, Japan*
[2)]*Kyushu Institute of Technology, Kitakyushu, Japan*

(Received June 24th, 2013)

The effects of density, thickness and heat load upon the heat shield performance of the lightweight phenolic carbon ablators named LATS (Lightweight Ablator series for Transfer vehicle Systems) were examined quantitatively for both arc-heated test and re-entry heating conditions using a one-dimensional ablation analysis code. Thermal conductivity values of the ablator were tuned based on the arc-heated test results by matching the calculated temperatures to the measured data. Main findings are: (1) For both heating conditions, the heat shielding performance of the ablator has the same tendencies with respect to parameters of the ablator density, thickness and heat load. (2) The dependency of the back surface temperature upon the ablator density is small especially for a large ablator thickness. (3) The surface recession decreases with the increase of the density. However, the mass loss increases almost linearly with the increase of the density. (4) The ablator necessary thickness, with which the maximum back surface temperature equals to the pre-determined allowable temperature value, is nearly constant as the density changes. The ablator necessary mass increases almost linearly, with the increase of the density. (5) In considering the mechanism of nearly equal necessary thickness of the ablator, it is very important that the thermal diffusivity does not vary much with different densities of the LATS ablator. (6) From the point of the reduction of the ablator weight, the selection of a lower density ablator is more advantageous than that of a higher density ablator.

Key Words: Ablator, Heat Shield System, Re-Entry Capsule, Ablation Analysis

Nomenclature

A_k : collision frequency, 1/s
B_k : activation temperature, K
C : constant value
C_p : specific heat, J/(kg K)
C_1 : tuning coefficient for thermal conductivity of virgin material
C_2 : tuning coefficient for thermal conductivity of char material
f_k : weighting factor
h : enthalpy, J/kg
k : thermal conductivity, W/(m K)
L : length of ablator, m
$\dot{m}$: mass loss rate, kg/(m^2 s)
Q : accumulated heat load, J/m^2
q : heat flux, MW/m^2
q_{max} : maximum heat flux, MW/m^2
$\dot{q}$: heat flux, W/m^2
$\dot{q}_{cw}$: cold wall convective heat flux, W/m^2
$\dot{q}_{net}$: net heat flux, W/m^2
RT : room temperature, K
$\dot{S}$: surface recession rate, m/s
T : temperature, K
T_{b_max} : maximum back surface temperature, K
T_s : surface temperature, K
t : thickness of ablator, m
x : moving coordinate or in-depth distance from receding surface, y-ΔS, m
y : stationary coordinate or in-depth distance from initial front surface, m
Δh_{pyro} : heat of pyrolysis per gas produced, J/kg
Δm : mass loss, kg/m^2
ΔS : surface recession, m
α : thermal diffusivity, m^2/s
ε : surface emissivity
ϕ_{blow} : blowing correction factor
μ_k : reaction order
ρ : density, kg/m^3
σ : Stefan-Boltzmann constant, 5.67×10^{-8} W/(m^2 K^4)
ω : $(\rho-\rho_{ch})/(\rho_v-\rho_{ch})$

Subscripts

ab : ablation
ch : char
g : pyrolysis gas
ne : necessary
PICA : phenolic impregnated carbon ablator
r : recovery
re : re-entry
ref : reference
u : at wall underside
v : virgin material
w : at wall

1. Introduction

A re-entry capsule has a heat shield system to protect inner equipments against severe heating environments during re-entry. The heat shield system is mainly consisted of an ablator which has a capability to prevent conduction of heat to the inside by an ablation phenomenon. Various kinds of ablative materials with various densities have been developed. Among them, the phenolic carbon ablator has been applied to the earth re-entry capsules such as USERS REV capsule (Unmanned Space Experiment Recovery System REcovery Vehicle)[1] and "Hayabusa" re-entry capsule[2] or the planetary entry probe "Gallileo" of NASA.[3] Each of these capsules used a high density ablator with the value of about 1500kg/m^3. A lightweight ablator of about 300kg/m^3 has also been developed[4] and used for the heat protection of the Stardust Capsule of NASA.[5]

Heat shield performance of the ablator depends on its density, thickness and heat load. For the design of a heat shield system, it is very important to evaluate quantitatively the ablator performance with respect to its density, thickness and heat load.

Recently, a lightweight ablator named LATS (Lightweight Ablator series for Transfer vehicle Systems) with the densities of about 300-700kg/m^3 has been developed.[6, 7] The LATS is a carbon phenolic ablator fabricated by impregnating a phenolic resin into a felt made of carbon fibers. The material properties of the LATS ablator were measured and arc-heated tests of the ablator samples with various densities were carried out. Measured in-depth temperatures agreed to the calculated results using a one-dimensional ablation analysis code.[8]

In this paper, the effects of density, thickness and heat load on the heat shielding performance of the LATS ablators are examined quantitatively using the one-dimensional ablation analysis code. Ablation analysis of the ablator with various thicknesses and densities of about 300-1000kg/m^3 was carried out using the one-dimensional ablation analysis code. Heat flux conditions of an arc-heated test and a typical earth re-entry vehicle were used for the calculation. Based on the above calculations, heat shielding performance (surface recession, mass loss, the back surface temperature, etc.) of the LATS ablators of various densities and thicknesses for various heating conditions was obtained and evaluated.

The study results would give important information in selecting the candidate ablator used for the heat shield system of a newly developed re-entry capsule in the near future.

2. Analysis

2.1. Method of analysis

We carried out one-dimensional ablation analysis of the LATS ablators with various densities and thicknesses for two kinds of heating conditions of arc-heated test and earth re-entry, from which the heat resistant performance of the LATS ablator with respect to the density, thickness and heat load was evaluated quantitatively. The flow of the study is shown in Fig. 1. The method of analysis carried out in this paper is basically the same as that used in the previous paper[8], except that the tuning parameters of C_1 and C_2 for thermal conductivity are based on the fitting lines described in section 2.5 in this study.

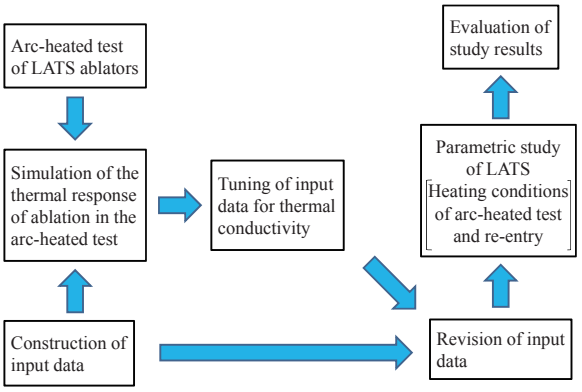

Fig. 1. Study flow.

2.2. Mathematical model of ablation[8]

A one-dimensional computer code for charring ablation and thermal response analysis was used to calculate the heat resistant performance of the LATS ablators. The code was developed for simulation of one-dimensional transient thermal behavior of charring materials, and was successfully applied to the LATS ablators under the heating environments of arc-heated test.[8] The mathematical model used in the code is described precisely in the previous papers.[8, 9] In the following, the basic equations and boundary condition are briefly described.

The basic equations about the charring ablation are well known.[8–13] Among the basic equations that this analysis code uses, the in-depth energy equation of the ablator is expressed by

$$\rho C_{\mathrm{p}} \left.\frac{\partial T}{\partial t}\right|_x = \frac{\partial}{\partial x}\left(k\frac{\partial T}{\partial x}\right)_t + \Delta h_{\mathrm{pyro}} \left.\frac{\partial \rho}{\partial t}\right|_y + \dot{S}\rho C_{\mathrm{p}} \left.\frac{\partial T}{\partial x}\right|_t + \dot{m}_{\mathrm{g}} \left.\frac{\partial h_g}{\partial x}\right|_t \tag{1}$$

where x is the coordinate with the origin fixed to the surface which moves due to the surface recession, y is the coordinate with the origin fixed to the ablator surface before heating, ρ is the density (kg/m^3), C_{p} is the specific heat (J/kg/K), T is the temperature (K), t is the time (s), k is the thermal conductivity (W/m/K), Δh_{pyro} is the heat of pyrolysis per produced gas of unit mass (J/kg), $\dot{S}$ is the surface recession rate (m/s), $\dot{m}_{\mathrm{g}}$ is the gas flow rate (kg/m^2/s) (mass flux) and h_g is the enthalpy of the pyrolysis gas (J/kg). k and C_{p} is calculated by

$$k = k_{\mathrm{v}}\omega + (1-\omega)k_{\mathrm{ch}} \quad \omega = (\rho - \rho_{\mathrm{ch}})/(\rho_{\mathrm{v}} - \rho_{\mathrm{ch}}) \tag{2}$$

$$\rho C_{\mathrm{p}} = \omega\rho_{\mathrm{v}} C_{\mathrm{pv}} + (1-\omega)\rho_{\mathrm{ch}} C_{\mathrm{pch}} \tag{3}$$

where ρ_{v} and ρ_{ch} are the virgin and char densities, k_{v} and k_{ch} are the thermal conductivities of the virgin and char materials, and C_{pv} and C_{pch} are the specific heats of the virgin and char materials, respectively.

The equation of mass conservation when the ablator yields the pyrolysis gas and the Arrhenius type expression for the decomposition rate are described by the following equations, respectively

$$(\partial \dot{m}_g / \partial y)_t = (\partial \rho / \partial t)_y \tag{4}$$

$$\left(\frac{\partial \rho}{\partial t}\right)_y = -\sum_{k=1}^{N} A_k f_k (\rho_v - \rho_{ch}) \left(\frac{\rho - \rho_{ch}}{\rho_v - \rho_{ch}}\right)^{\mu_k} \exp\left(-\frac{B_k}{T}\right) \quad (5)$$

where μ_k is the reaction order, A_k is the weighting factor, f_k is the collision frequency (1/s), B_k is the activation temperature (K). These values are assumed to be constant.

The energy balance at the ablator surface yields the surface boundary condition. In consideration of aerodynamic heating, block effect of heating due to the gas ejection, radiation cooling, and enthalpy change when the char recedes, enthalpy change of pyrolysis gas and the heat conduction in the ablator, the energy balance equation is obtained and shown below, [12]

$$\dot{q}_{net} = \dot{q}_{cw}(1 - h_w/h_r)\phi_{blow} - \varepsilon\sigma(T_w^4 - T_{ref}^4) - \dot{m}_{ab}(h_w - h_u) \quad (6)$$

where $\dot{q}_{net}$ is the net heat flux conducted into the ablator (W/m^2), $\dot{q}_{cw}$ is the cold wall convective heat flux (W/m^2), h_w is the enthalpy of the gas adjacent to the surface, h_r is the recovery enthalpy of the flow, ϕ_{blow} is the blowing correction factor, ε is the emissivity, σ is the Stefan-Boltzmann constant (5.670×10^{-8} W/m^2/K^4), T_w is the temperature of the char surface (K), T_{ref} is 300 K, $\dot{m}_{ab}$ ($=\rho_{ch}\dot{S}$) is the mass flux due to the thermochemical ablation of the char (kg/m^2/s), and h_u is the enthalpy of the char at the surface (J/kg).

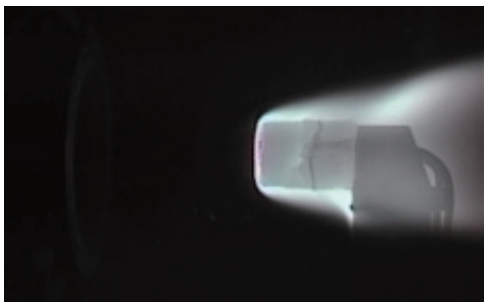

Fig. 2. Test model during arc-heated test.

2.3. Arc-heated test [8]

Arc-heated tests of the new low density phenolic carbon ablators called LATS (Lightweight Ablator series for Transfer Vehicle) were carried out using the 750 kW arc heating wind tunnel of Japan Aerospace Exploration Agency (JAXA). Each ablator test model had a cylindrical shape and the heating surface of the model was flat.

The tests were carried out with two kinds of heating conditions: one is the low heating rate of 0.97 MW/m^2, with the impact pressure of 1930 Pa and the flow enthalpy of 12.8 MJ/kg, and the other is the high heating rate of 1.98 MW/m^2, with the impact pressure of 4250 Pa and the flow enthalpy of 18.8 MJ/kg, where air was used as a working gas. The heating time was mainly 60s. The time history of the in-depth temperature was measured for 600s, where the start time of the heating corresponds to 0s. A test model during the arc-heated test is shown in Fig. 2. The flat surface of the test model is heated by the high-enthalpy flow, which is ejected from the nozzle on the left of the model in the figure. The diameter and length of the test model are 34 mmϕ and 20mm, respectively.

The surface temperature of the test model was measured by the two-color pyrometer and the in-depth temperature was measured by K type thermocouples installed in the ablator.

2.4. Input data of material properties [8]

The input data for the calculation of the thermal behavior of the test model using the one-dimensional ablation analysis program include parameters such as heating environment conditions, ablator thickness and material properties. The virgin density ρ_v of the ablator are set based on the measurement of each model. The char density for each ablator model is calculated by means of the following relation based on the measurement of virgin and charred materials. [7]

$$\rho_{ch} = \rho_v \times 0.7 \quad (7)$$

The emissivity of the char surface was set to be 0.85. [8, 12]

The reference value of thermal conductivity of the virgin material k_{vref} is constructed of the measured value of the LATS materials with the density of about 300 kg/m^3, using a steady-state method with the temperature range from room temperature (RT) to 573 K (300 ºC), combined with the literature data [4] of the low density (about 300 kg/m^3) ablator (PICA) multiplied by a constant value, $C*k_{vPICA}(T)$, where $k_{vPICA}(T)$ is the thermal conductivity of the PICA and C is a constant value that is determined so that the two data are smoothly connected. The reference value of thermal conductivity of the char material k_{chref} is assumed to be the same as that of the virgin material k_{vref} (k_{chref}=k_{vref}).

The specific heat of the char material C_{pch} is based on the following expression[12]

$$C_{pch} = C_\infty \frac{T}{\sqrt{T^2 + D^2}} \quad (8)$$

where T is the temperature (K), $C_\infty = 2.3 \times 10^3$ J/(kg K), and D = 800 K. The specific heat of the virgin material C_{pv} is constructed of the measured data with the temperature range of RT to 300 ºC (573 K), combined with Eq. (8), in which the connection is made smoothly.

The specific heat of the pyrolysis gas C_{pg} is set to be a constant value of 1674.6 J/(kg·K).[13] The heat of pyrolysis per gas produced Δh_{pyro} is set to be 3.313×10^5 J/kg (79.1 cal/g), which is determined considering the measured and the literature data. Coefficients in the Arrhenius equation (Eq. (5)) are set based on the TGA data of the LATS ablator.[14] Values of N = 2, A_1 = 0.1, $f_1 = 3.5 \times 10^9$ 1/s, B_1 = 1.1*10^4 K, μ_1 = 100.0, A_2 = 0.9, f_2 = 7.0*10^3 1/s, B_2 = 1.1×10^4 K, μ_2 = 3 are used in the calculation.

2.5. Tuning of input data [8]

Among the input data for the simulation of the LATS ablator mentioned above, thermal conductivity values would have a large effect on the temperature calculation. However, we have not yet obtained a sufficient amount of reliable measured data of thermal conductivity for the LATS material, especially in a high temperature region. Moreover the thermal conductivity not only depends on the temperature but also on the ablator density.[14] In order to overcome this difficulty, tuning of the thermal conductivity by matching the calculated

temperatures to the measured data was carried out for the simulation. The procedure of the tuning method is shown as follows:

(1) Multiply the thermal conductivity data k_{vref} and k_{chref} by appropriate constant values of the tuning coefficients C_1, C_2 to yield a new set of thermal conductivity C_1*k_{vref} and C_2*k_{chref}.

(2) Using the new set of C_1*k_{vref} and C_2*k_{chref}, we carry out the ablation analysis.

(3) If the calculated temperatures do not agree well with the measured results, the tuning coefficients C_1, C_2 are changed and ablation analysis is carried out using the changed values of C_1, C_2.

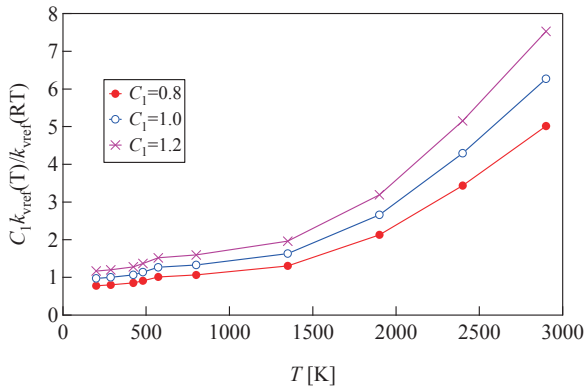

Fig. 3. Relation between $C_1k_v(T)/k_{vref}(RT)$ and temparature for tuning.

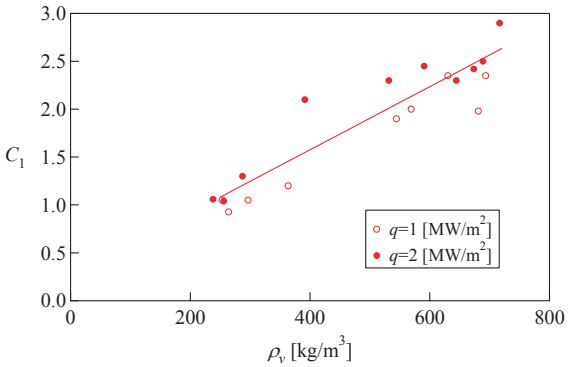

Fig. 4. Relation between C_1 and virgin density.

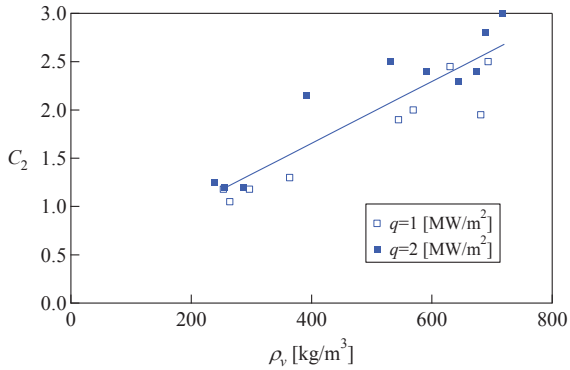

Fig. 5. Relation between C_2 and virgin density.

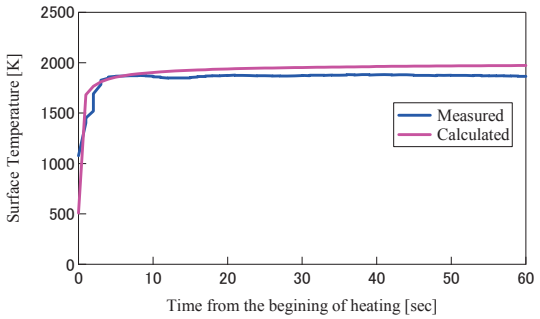

Fig. 6. Comparison of surface temparatures.
(ρ_v=253.4 kg/m^3, q =0.97 MW/m^2, C_1=1.05, C_2=1.18)

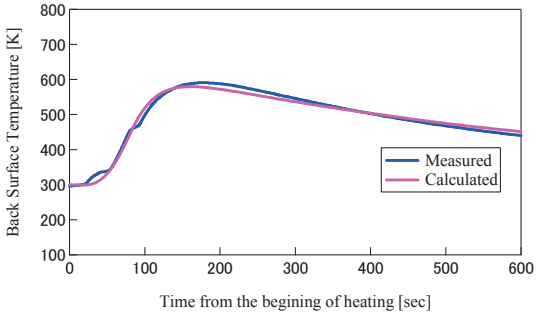

Fig. 7. Comparison of back surface temparatures.
(ρ_v=253.4 kg/m^3, q =0.97 MW/m^2, C_1=1.05, C_2=1.18)

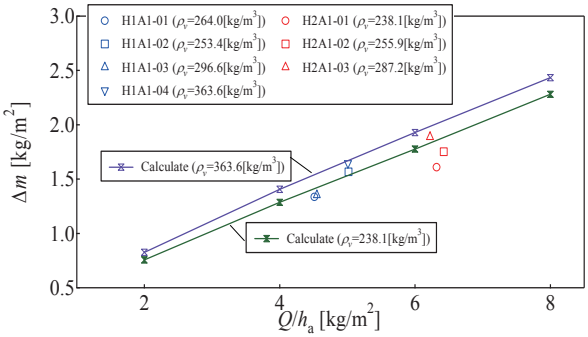

Fig. 8. Relation between mass loss and Q/h_a.

(4)The procedure (3) is continued until we have a good agreement between calculation and measurement.

(5) When the calculated temperature agrees well with the measured temperature, the tuning coefficients C_1, C_2 are finally determined.

Figure 3 shows the thermal conductivity $C_1k_{vref}(T)/k_{vref}(RT)$, where $k_{vref}(RT)$ is the reference value of thermal conductivity at RT (k_{vref} is defined in section 2.4). In the figure, curves corresponding to C_1=0.8, 1.0 and 1.2 are shown. The tuning coefficients C_1 and C_2, each of which was obtained for each test, are plotted in Figs. 4 and 5. Approximate lines obtained by the least square method for C_1 and C_2 are also shown in these figures. Values of C_1 and C_2 described by the approximate lines were used in the ablation analysis, respectively.

Figures 6 and 7 show examples of matching results of the

LATS ablator. Relatively good agreement of the temperatures is obtained. It is seen that the simulation results of the surface and the back surface temperature time histories by the analysis program agree well with the measured results. Figure 8 shows the relation between the mass loss Δm and Q/h_a, where Q is the heat load [J/m^2] and h_a is the air enthalpy [J/kg]. It is seen that the simulation results of mass loss Δm by the analysis program agree well with the measured results.

2.6. Parametric study

Ablation analysis of the ablator system was carried out for two kinds of heating environments of arc-heated test and re-entry. Back surface temperatures T_b [K], mass loss Δm [kg/m^2] and surface recession ΔS [m] are calculated as functions of virgin density ρ_v [kg/m^3], ablator thickness t [m] and heat flux q [MW/m^2]. The necessary thickness t_{ne} [m] and mass m_{ne} [kg/m^2] are also calculated as functions of ρ_v and q. The necessary thickness or mass is defined to be the thickness or mass per unit area in which the maximum back surface temperature of the ablator is equal to a pre-determined allowable value of temperature (bond line temperature). In this paper we used a value of 250C^O (=523.15K=480F) for the bond line temperature.[15)]

For the calculation under the arc-heated test conditions, heating rate time histories of a rectangular pattern were used, which is shown in Fig. 9a. The impact pressure of 1930 Pa and enthalpy of 12.8 MJ/m^2, the values of which are the same

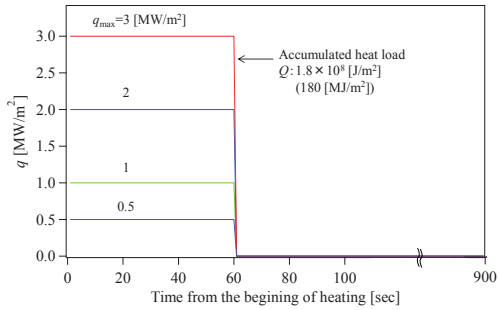

Fig. 9a. Heating rate for arc-heated test.

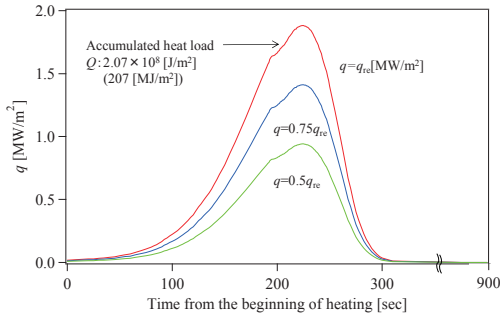

Fig. 9b. Heating rate for re-entry.

as those of the arc-heated test described in section 2.3, are used for the calculation. For each pattern of the heating time histories, the heating rate q keeps a constant value (a constant maximum value q_{max}) from 0 to 60s.

For the calculation under the re-entry conditions, heating rate q expressed by q=Cq_{re} were used, where C is a constant value and q_{re} is the re-entry heating rate of USERS/REV at the stagnation point.[16)] The heating rate q_{re} was calculated based on the correlation formula for the stagnation heat transfer rate to a blunt body of revolution in hypersonic flow.[17)] The enthalpy and impact pressure used in the calculation were the same as those in the re-entry environment of USERS/REV.[16)] The heating rate time histories used for the calculation of re-entry are shown in Fig. 9b.

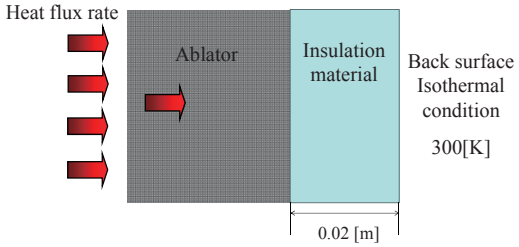

Fig. 10. Thermal model for the analysis.

Figure 10 shows the thermal model used in the analysis for both heating conditions. It was assumed that an insulation material (fibrous insulation material) with a thickness of 20mm, a density of 125 kg/m^3, and a thermal conductivity of 0.011 W/(mK) at RT was attached to the back of the ablator. As a boundary condition, the temperature at the back surface of the insulation material was assumed to be a constant value of 300K.

Other kinds of adiabatic and radiative back surface conditions (in the radiative condition, heat is transferred to the inner side by radiation), were also considered. Some calculations were carried out with these conditions, the results of which were nearly the same as those with the isothermal condition. For this reason, only the results with the isothermal condition are shown, in this paper.

Calculations were carried out until the time of 900s for both heating conditions. The time of 900s approximately corresponds to the splash down time of the USERS REV capsule. Parameters of mass loss Δm and surface recession ΔS were evaluated at time t=900s. The maximum back surface temperature T_{b_max} was evaluated between the times of 0s and 900s. The necessary thickness t_{ne} and mass m_{ne} were evaluated at the time corresponding to T_{b_max}.

3 Results and Discussion

3.1. Maximum back surface temperature T_{b_max}

Figures 11a and 11b show the relations between ρ_v and T_{b_max} with two kinds of ablator thicknesses t and heating rate q for two kinds of heating conditions, respectively. It is seen that T_{b_max} increases with the increase of q or decrease of t. In both figures, it is also seen that the dependency of T_{b_max} upon ρ_v is smaller when q is lower and t is larger.

As described in section 3.4, it seems that the back surface temperature is largely influenced by the parameters of thermal diffusivity α, ablator length L (or surface recession ΔS) and surface temperature T_s. A combination of these parameters may determine the back surface temperatures of the LATS ablators with different densities. The precise mechanism

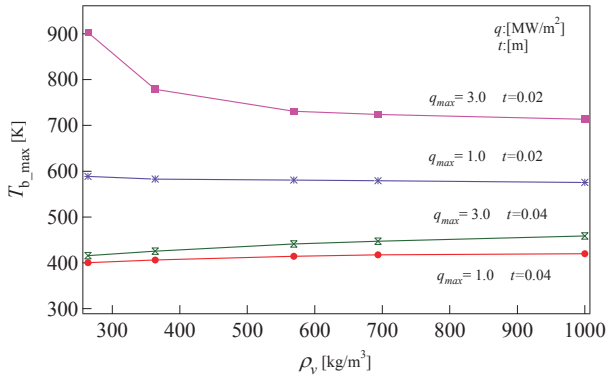

Fig. 11a. Relation between maximum back surface temperature and virgin density for arc-heated test conditions.

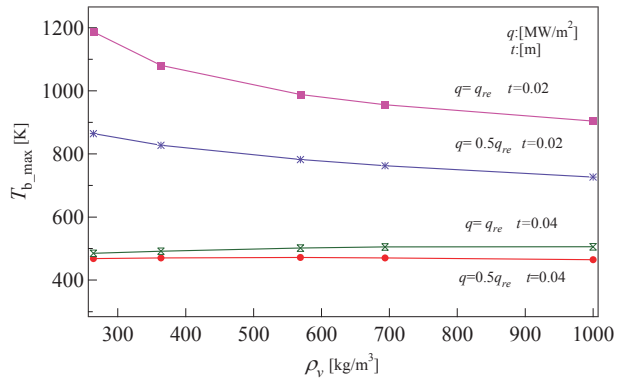

Fig. 11b. Relation between maximum back surface temperature and virgin density for re-entry conditons.

which determines the back surface temperature is suggested in section 3.4.

3.2. Mass loss of ablator Δ*m*

Figures 12a and 12b show the relations between the mass loss Δ*m* and the ablator density ρ_v with several kinds of *q* and *t* for the two kinds of heating conditions, respectively. It is seen that Δ*m* increases as *q* increases, and the dependency of Δ*m* upon the ablator thickness *t* is small. It is also seen that for both heating conditions, Δ*m* increases as ρ_v increases, and the relation is nearly linear.

As for the relation between Δ*m* and ρ_v, this can be explained simply by using a simple model, which is described

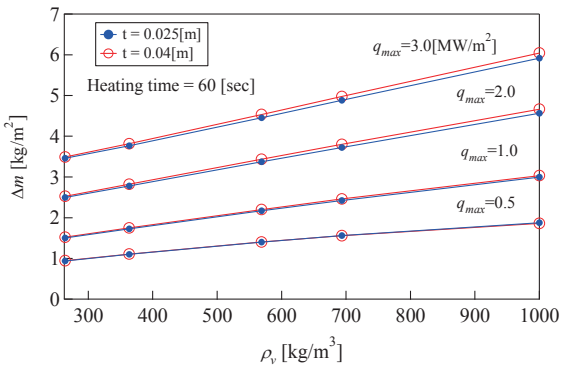

Fig. 12a. Relation between mass loss and virgin density for arc-heated test conditions.

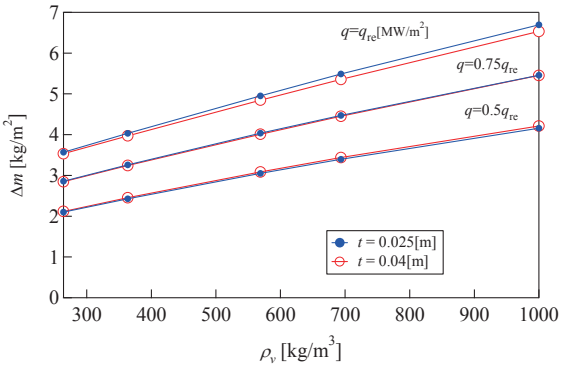

Fig. 12b. Relation between mass loss and virgin density for re-entry conditions.

as follows:

It is assumed that a heated ablator (1) consists of the charred region with the length of L_{ch1} and the density of ρ_{ch1}, and the virgin region with the density of ρ_{v1}. Then, the mass loss Δm_1 is expressed by

$$\Delta m_1 = \Delta S_1 \rho_{v1} + L_{ch1}(\rho_{v1} - \rho_{ch1}) \tag{9}$$

where ΔS_1 is the surface recession of the ablator(1). Substituting Eq. (7) into Eq. (9) yields

$$\Delta m_1 = \Delta S_1 \rho_{v1} + 0.3 L_{ch1} \rho_{v1} \tag{10}$$

As for an ablator (2), the same relation can also be applied. We assume that the char removal is mainly due to diffusion controlled oxidation[9, 12] and the amount of oxygen diffused into the ablator is determined by the heating rate. We also assume that the amount of char removal is determined by the amount of oxygen diffused into the ablator surface. Then the amount of char removal of an ablator is the same for the same heating conditions. Then the following relation is obtained.

$$\Delta S_1 \rho_{ch1} = \Delta S_2 \rho_{ch2} \tag{11}a$$

$$\Delta S_1 \rho_{v1} = \Delta S_2 \rho_{v2} \tag{11}b$$

By using the above equations, Δm_1-Δm_2 is given by

$$\Delta m_1 - \Delta m_2 = \Delta S_1 \rho_{v1} - \Delta S_2 \rho_{v2} + 0.3 L_{ch1} \rho_{v1} - 0.3 L_{ch2} \rho_{v2} \tag{12}$$

By using Eq. (11)b and assuming that both of the char depth L_{ch1} and L_{ch2} are equal, the following relation is obtained.

$$\Delta m_1 - \Delta m_2 = 0.3 L_{ch1}(\rho_{v1} - \rho_{v2}) \tag{13}$$

The above equation shows that the difference of the mass loss is proportional to the difference of the density. This means that Δ*m* increases as ρ_v increases linearly. Although the assumption of the above model is rather simplified, the results are similar to those of the ablation analysis. It seems that this model can express the main mechanism of mass loss rather well.

Figure 12c shows an example of calculated time dependent density distributions of the ablator of ρ_v=1000kg/m^3 for the re-entry condition of $q=q_{re}$. In this paper it is tentatively defined that the virgin zone is that of $\rho/\rho_v > 0.95$, and the char and pyrolysis zones are those of $\rho/\rho_v < 0.95$. With this definition of zones, it is seen that the thickness of the virgin

zone is about 1/2 of the overall thickness. It seems that in this case the thermal property of the material in the virgin zone influences the increase of the ablator back surface temperature, necessary thickness and necessary mass.

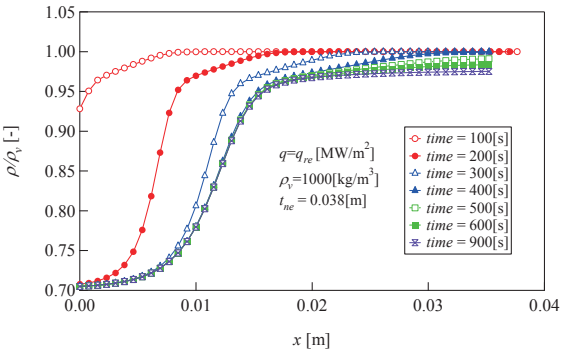

Fig. 12c. Time dependent density distribution.

3.3. Surface recession ΔS

Figures 13a and 13b show the relations between the surface recession of the ablator ΔS and the virgin density ρ_v with several kinds of q and t for two kinds of heating conditions, respectively. For both heating conditions, ΔS increases with the decrease of ρ_v or the increase of q. The dependency of ΔS upon the thickness t is almost zero.

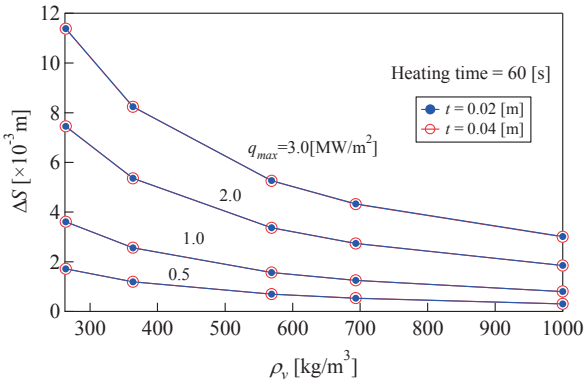

Fig. 13a. Relation between surface recession and virgin density for arc-heated test conditions.

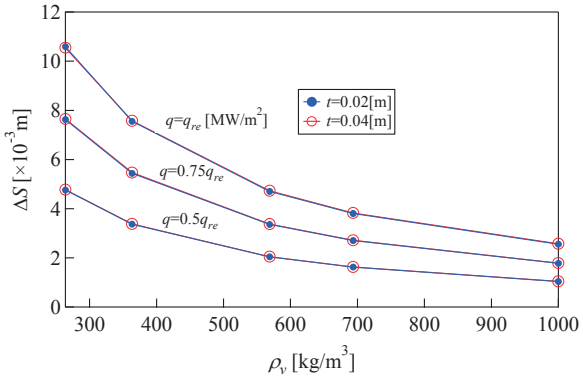

Fig. 13b. Relation between surface recession and virgin density for re-entry conditions.

3.4 Necessary thickness t_{ne}

Figures 14a and 14b show the relations between the necessary thickness of the ablator t_{ne} and the virgin density ρ_v with various q for two kinds of heating conditions, respectively. (Necessary thickness t_{ne} is defined in section 2.6) The necessary thickness t_{ne} increases with the increase of q. It is also seen that for both heating conditions, the dependency of t_{ne} upon ρ_v is very small. The same or nearly equal values of t_{ne} means the same or nearly equal values of the maximum back surface temperature T_{b_max} of the ablator.

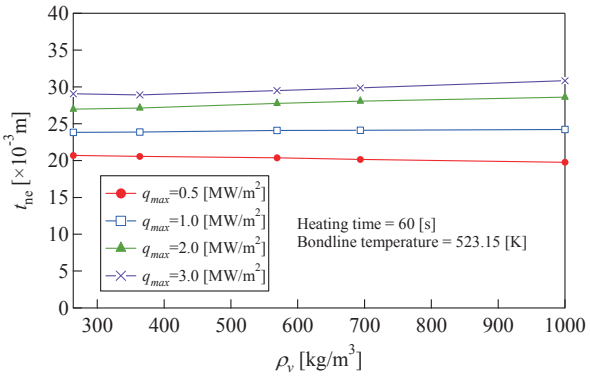

Fig. 14a. Relation between necessary thickness of ablator and virgin density for arc-heated test conditions.

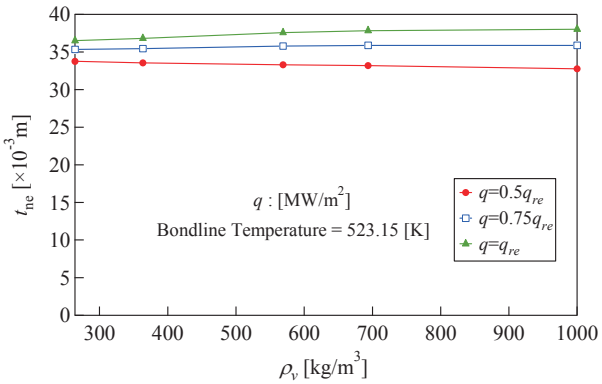

Fig. 14b. Relation between necessary thickness of ablator and virgin density for re-entry conditions.

For one-dimensional non-ablating materials under the unsteady-state conduction heat transfer, the in-depth temperature depends on the non-dimensional parameter of $\alpha\,\theta/L^2$ [θ: time, s] under the same initial and temperature boundary conditions.[18] The same values of α and the length L, and the same initial and temperature boundary conditions yield the same transient temperature distributions. When α or the surface temperature T_s increase, or L decreases, the in-depth temperature increases. By assuming that this tendency is also applicable to the ablative materials, we try to explain the relation between t_{ne} and ρ_v by means of the parameters of α, L and T_s. The back surface temperature of the ablator is influenced by the parameters of α, L, and T_s (or $\alpha\,\theta/L^2$).

1) Thermal diffusivity α

When α becomes larger, the back surface temperature increases or decreases rapidly. The differences of the thermal diffusivity of the LATS virgin and char materials of different

densities are less than 30%. That is to say, the differences of thermal diffusivity α among the ablators are small. The thermal diffusivity of a low density LATS ablator is a little larger than that of a high density ablator. From the point of α, the back surface temperature of a lower density ablator increases or decreases easily compared with a higher density ablator.

2) Ablator thickness L (surface recession ΔS)

The back surface temperature varies with $1/L^2$. If the ablator thickness decreases due to surface recession during heating, the back surface temperature would increase, which means that the increase rate of the temperature increases. After the heating is finished, the surface temperature decreases, and the back surface temperature tends to decrease. The decreasing rate of the temperature is larger when L becomes smaller. This means that from the point of surface recession the back surface temperature of a lower density ablator, which suffers more surface recession, tends to increase or decrease more rapidly compared with a higher density ablator.

3) Surface temperature T_s

When the surface temperature is larger or smaller, the back surface temperature would be larger or smaller, respectively. The surface temperature of a lower density ablator is a little higher than that of a higher density ablator during heating, and a little lower than that of a higher density after heating is finished. (This tendency is confirmed by calculation. This may be due to the heat capacity of the ablators.) Then, the back surface temperature of a lower density ablator becomes a little higher than that of a higher density ablator due to the surface temperature increase because of the heating, and becomes a little lower than that of a higher density due to the cooling down of the surface temperature after heating is finished. From the point of the surface temperature, the back surface temperature of a lower density ablator increases or decreases easily, compared with a higher density ablator.

Based on the above discussion, the reason why t_{ne} is nearly equal for different densities is examined in the following:

From the point of α, L and T_s during the heating, the surface temperature and the back surface temperature of a lower density ablator increase higher than that of a higher density ablator. However, after the heating is finished, the surface temperature of the lower density ablator becomes lower compared with the higher density ablator, and the rate of the cooling down of the back surface temperature becomes higher. Although the increasing rate of the back surface temperature of a lower density ablator is higher, the decreasing rate is also higher compared with that of a higher density ablator. Conversely, while the increasing rate of the back surface temperature of a higher density ablator is lower, the decreasing rate is also lower compared with that of a lower density ablator.

The combination of these mechanisms of the ablator thermal behavior gives nearly equal back surface temperatures for different density ablators. Among these thermal characteristics of the LATS ablator, a very important item which contributes to the relation of t_{ne} and ρ_v would be that the thermal diffusivity α of the LATS is nearly equal for different densities. This may explain the reason why t_{ne} is nearly equal for different densities.

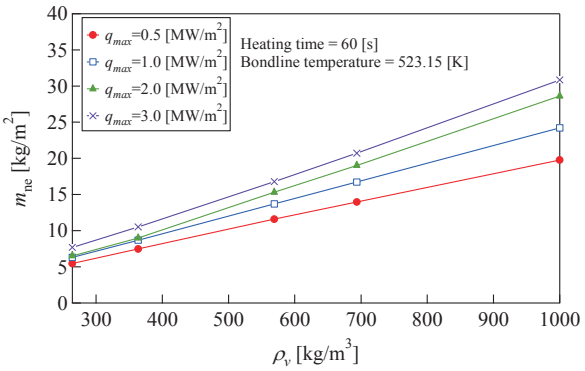

Fig. 15a. Relation between necessary mass and virgin density for arc-heated test conditions.

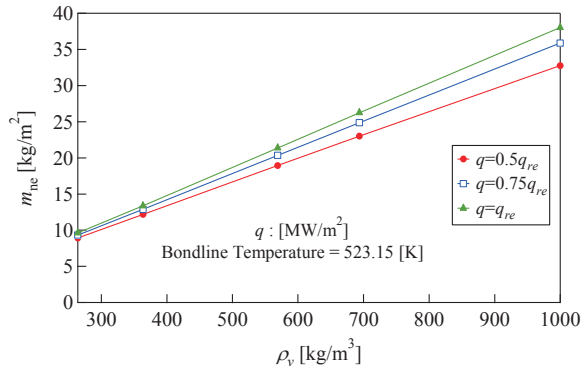

Fig. 15b. Relation between necessary mass and virgin density for re-entry conditions.

By means of these parameters, the behavior of T_{b_max} in Figs. 11a-11b can be explained as follows:

In both figures, it is seen that, in the case of high q and small t, T_{b_max} becomes higher when ρ_v is lower. When ρ_v is lower , ΔS becomes larger and t-ΔS becomes much smaller. Moreover, when ρ_v is lower, α is larger and T_s is higher during heating. These factors tend to increase T_{b_max} of a low density ablator. Then the maximum back surface temperature T_{b_max} decreases as ρ_v increases.

When the ablator thickness t is 40mm, the T_{b_max} curves are relatively flat. For most of the curves, the T_{b_max} curve increases slightly, as ρ_v increases. When t is thick, t-ΔS becomes not so small and the effect of t-ΔS, which tends to increase the maximum back surface temperature, becomes small. When ρ_v is higher, the effect of increasing T_b after the heating is finished becomes larger. The combination of these thermal behaviors gives a slightly larger value of T_{b_max} for a higher density ablator.

3.5. Necessary mass m_{ne}

Figures 15a and 15b show the relations between the necessary mass of the ablator m_{ne} and the virgin density ρ_v with various q for two kinds of heating conditions, respectively. It is seen that for both heating conditions, the necessary mass increases as ρ_v increases, and the relation is nearly linear. It is also seen that m_{ne} increases as q increases. (The necessary mass m_{ne} is defined in section 2.6)

It is found that in order to satisfy the back surface temperature requirement, selection of a lower density ablator is more advantageous than that of a higher density ablator from the point of reducing the ablator weight.

3.6. Effect of material parameters

The tuning coefficients C_1 and C_2 for ablator thermal conductivity shown in Figs. 4 and 5 are seen to scatter around the approximate lines. In order to examine the effects of scatter upon the necessary thickness t_{ne} and mass m_{ne}, ablation analysis was carried out. The values of C_1 and C_2 were varied from 0.75 to 1.35 of those of the approximate lines, respectively, in which the parameter ranges of C_1 and C_2 were determined so that they include the scatter. The calculation results show that when C_1 and C_2 change from 0.75 to 1.35 of the values of approximate lines, the deviations of t_{ne} change from -0.17 to 0.2 of the values shown in Figs 14a and 14b, and the deviations of m_{ne} change from -0.17 to 0.2 of the values shown in Figs 15a and 15b, with the ablator densities from 264 to 1000kg/m^3 for both arc-heated test and re-entry conditions. The effects are found to be not so large.

The effects of parameters (thickness, density and thermal conductivity) of the insulation material upon t_{ne} and m_{ne} were also investigated. The calculation results show that when the thickness, density and thermal conductivity of the insulation change from 0.5 to 2.0 of the values described in section 2.6, the deviations of t_{ne} and m_{ne} change within ± 0.04 of the values in Figs.14a-15b, respectively, with the ablator densities from 264 to 1000kg/m^3 for both arc-heated test and re-entry conditions. The effects are found to be small.

There are various kinds of ablators which have been developed and studied so far.[12, 19-24] They have different values of thermal diffusivity. If an ablator is a phenolic carbon ablator (CFRP type), the ablation mechanism is similar to that of the LATS ablator. Moreover, if the thermal diffusivity is nearly equal to that of the LATS, the tendency of thermal protection performance would be similar to that of the LATS. If an ablator is not of a CFRP type, the ablation mechanism would be different from that of the CFRP ablator. It is not clear whether the tendency of thermal protection performance is similar to that of the LATS ablator or not, even if the thermal properties (for example, especially thermal diffusivity) are similar to those of the LATS ablator. A new study would be necessary to make this clear.

When the thermal diffusivity of an ablator is lower, the back surface temperature becomes lower, which contributes to the ablator weight reduction.

3.7. Effect of heating environment

If the heat load and the maximum heat flux rate applied on the ablator are within the range treated in this paper, the tendency of thermal protection performance of the LATS ablator would be similar to that described in this section. The surface temperature of the ablator calculated in this paper is less than about 3000K and the surface ablation is mainly in the diffusion controlled oxidation or reaction control oxidation regions.[9, 12]

If the heating level is such that the surface ablation is in the sublimation region[12], where the surface temperature is higher than about 3000K, the surface recession becomes much larger than that in diffusion controlled oxidation or reaction control oxidation regions. In this case, it is not clear whether the tendency of thermal protection performance is similar to that of the LATS ablator described in this paper or not. A new study would be necessary to make this clear.

It is seen from the above discussion that the evaluation of the LATS ablator based on the arc-heated test conditions gives similar results to those based on the re-entry conditions.

4. Conclusions

The effects of density, thickness and heat load upon the heat shield performance of the lightweight phenolic carbon ablator of LATS (Lightweight Ablator series for Transfer vehicle Systems) were examined quantitatively for both arc-heated test and re-entry heating conditions using a one-dimensional ablation analysis code. Main findings within the range of parameters investigated are:

(1) For both arc-heated test and re-entry heating conditions, the heat shielding performance of the LATS ablator has the same tendencies with respect to parameters of the ablator density ρ_v, thickness t and heat load q. This means that the evaluation of the LATS ablator based on the arc-heated test conditions gives similar results to those based on the re-entry conditions.

(2) The dependency of the back surface temperature upon the ablator density is small especially for a large ablator thickness.

(3) The surface recession decreases with the increase of the density. The mass loss increases almost linearly with the increase of the density.

(4) The ablator necessary thickness, with which the maximum back surface temperature equals to the pre-determined allowable temperature value, is nearly constant as the density changes. The ablator necessary mass increases linearly, with the increase of the density.

(5) The mechanism of the nearly equal necessary thickness of the ablator was investigated. In considering the mechanism, it is very important that the thermal diffusivity does not vary much with different densities of the LATS ablator.

(6) The effects of material parameter variations of the ablator (thermal conductivity) and insulation material (thickness, density and thermal conductivity) upon the necessary thickness and mass were investigated. Within the range of parameters investigated, the effects were found to be not so large or small.

(7) From the point of the reduction of the ablator weight, the selection of a lower density ablator is more advantageous than that of a higher density ablator.

The study results would give important information in selecting the candidate ablator used for the heat shield system of a newly developed re-entry capsule in the near future.

Acknowledgement

The authors are deeply grateful to the people of KHI, JAXA and Nagoya Univ. for their support to our research.

References

1) Kato, S., Sakata, R., Kanno, Y., Uto, M., Okuyama, K., Uegaki, E., Shingu, S., Ijichi, K. and Inatani, Y.: Development of

USERS/REM Heat Shield System and its Evaluation after Re-entry, ISTS2004-e-36, Proceedings of the 24th International Symposium on Space Technology and Science (Selected Papers), Miyazaki, Japan, (2004), pp. 621-628.
2) Yamada, T., Ishii, N. and Inatani, Y.: Post Flight Analysis of the Hayabusa Sample Return Capsule, 2011-def-03, 28th International Symposium on Space Technology and Science (28th ISTS), 5-12 June, Okinawa Prefecture, Japan.
3) Milos, F. S., Chen, Y.-K. and Squire T. H.: Analysis of Galileo Probe Heat Shield Ablation and Temperature Data: Ablation and Thermal Response Program for Spacecraft Heatshield Analysis, Journal of Spacecraft and Rockets, **36** (1999), pp. 298-306.
4) Tran, H., Johnson, C., Rasky, D., Hui, F., Chan, Y. K. and Hsu, M.: Phenolic Impregnated Carbon Ablators (PICA) for Discovery Class Missions, AIAA-96-1911, 31st AIAA Thermophysics Conference, June 1996.
5) Kontinos, D. A. and Stackpoole, M.: Post Flight Analysis of the Stardust Sample Return Capsule Earth Entry, AIAA-2008-1197, 46th AIAA Aerospace Sciences Meeting and Exibit, Reno, Nevada, January, 2008.
6) Okuyama, K., Kanada, T., Kato, S., Sakai, T., Suzuki, T., Fujita, K. and Nishio, S.: Thermochemical and Thermomechanical Characteristics of an Ultra Lightweight CFRP under High Temperature Environments, 2011-c-15, 28th International Symposium on Space Technology and Science (28th ISTS), 5-12 June 2011, Okinawa Prefecture, Japan.
7) Okuyama, K., Kato, S. and Ohya, H.: Thermochemical Performance of a Lightweight Charring Carbon Fiber Reinforced Plastic, Transactions of the Japan Society for Aeronautical and Space Sciences. **56** (2013), pp.159-169.
8) Kato, S., Okuyama, K., Gibo, K., Miyagi, T., Suzuki, T., Fijita, K., Sakai, T., Nishio, S. and Watanabe, A.: Thermal Response Simulation of Ultra Light Weight Phenolic Carbon Ablator by the Use of the Ablation Analysis Code, Transactions of JSASS Aerospace Technology Japan, **10** (2012), pp.31-39.
9) Kato, S., Okuyama, K., Nisio, S., Sakata, R., Hama, K. and Inatani, Y.: Numerical Analysis of Charring Ablation for Ablative Materials of Re-Entry Capsules, Journal of the Japan Society for Aeronautical and Space Sciences, **50** (2002), pp. 255-263.(in Japanese)
10) Moyer, C. B. and Rinadal, R. A.: An Analysis of Coupled Chemically Reacting Boundary Layer and Charring Ablator, Part Ⅱ, Finite Difference Solution for the In-Depth Response of Charring Materials Considering Surface Chemical and Energy Balances, NASA CR-1061, 1967.
11) Chen, Y.-K. and Milos, F. S.: Ablation and Thermal Response Program for Spacecraft Heatshield Analysis, Journal of Spacecraft and Rockets, **36** (1999), pp. 475-483.
12) Potts, R, L: Application of Integral Methods to Ablation Charring Erosion, A Review, Journal of Spacecraft and Rockets, **32** (1995), pp. 200-209.
13) Potts, R, L.: Hybrid Integral/Quasi-Steady Solution of Charring Ablation, AIAA-90-1677, AIAA/ASME 5th Joint Thermophysics and Heat Transfer Conference, June 1990.
14) Suzuki, T., Fujita, K., Sakai, T., Okuyama K., Kato, S. and Nishio, S.: Thermal Response Analysis of Low Density CFRP Ablator, 2011-e-41, 28th International Symposium on Space Technology and Science (28th ISTS), 5-12 June 2011, Okinawa Prefecture, Japan.
15) Willcockson, W. H.: Mars Pathfinder Heatshield design and Flight Experience, Journal of Spacecraft and Rockets, **36** (1999), pp. 374-379.
16) Oya, K., Matsuda, S. and Ishii, N.: Reentry Flight and Attitude Motion of USERS Reentry Capsule, JAXA Research and Development Report, Research for the Development, and Post-Flight Analysis of the USERS REV Capsule. JAXA-RR-04-045, ISSN 1349-1113, Mar.(2005) pp.21-29. (in Japanese)
17) Detra, R. W., Kemp, N. H. and Riddell, F. R.: Addendum to Heat Transfer to Satellite Vehicles Re-entering the Atmosphere, Jet Propulsion, December (1957), pp1256-1257.
18) Holman, J. P., Heat Transfer, Ninth Edition, McGraw-Hill, 2002.
19) Peterson, D. L. and Nicoleit, W. E.: Heat Shielding for Venus Entry Probes, Journal of Spacecraft and Rockets, **11** (1974), pp. 382-387.
20) Tran, H., Johnson, C., Rasky, D., Hui, F., Chan, Y. K., Hsu, M., Chen, T., Chen, H. C., Jose, S., Paragas, D. and Kobayashi, L.: Phenolic Impregnated Carbon Ablators (PICA) as Thermal Protection Systems for Discovery Missions, Nasa Technical Memorandum 110440, April 1997.
21) Bueche, J. F.: Effects of improvements and uncertainties in thermophysical properties on carbon phenolic heatshield thermal performance, AIAA-787.
22) Sutton, K.: An experimental study of a carbon-phenolic ablation material, NASA TN D-5930, Sept. 1970.
23) Moyer, C. B. and Green, K. A.: Demonstration of the Range over which the Langley Research Center Digital Computer Charring Ablation Program (CHAP) can be Used with Confidence, Comparisons of CHAP Predictions and Test Data for Three Ablation Materials, NASA CR-1980, Feb. 1972.
24) Strauss, E. L.: Superlight Ablative Systems for Mars Lander Thermal Protection, Journal of Spacecraft and Rockets, **4** (1967), pp.1304-1309.